

RSC Advances



This is an *Accepted Manuscript*, which has been through the Royal Society of Chemistry peer review process and has been accepted for publication.

Accepted Manuscripts are published online shortly after acceptance, before technical editing, formatting and proof reading. Using this free service, authors can make their results available to the community, in citable form, before we publish the edited article. This *Accepted Manuscript* will be replaced by the edited, formatted and paginated article as soon as this is available.

You can find more information about *Accepted Manuscripts* in the [Information for Authors](#).

Please note that technical editing may introduce minor changes to the text and/or graphics, which may alter content. The journal's standard [Terms & Conditions](#) and the [Ethical guidelines](#) still apply. In no event shall the Royal Society of Chemistry be held responsible for any errors or omissions in this *Accepted Manuscript* or any consequences arising from the use of any information it contains.

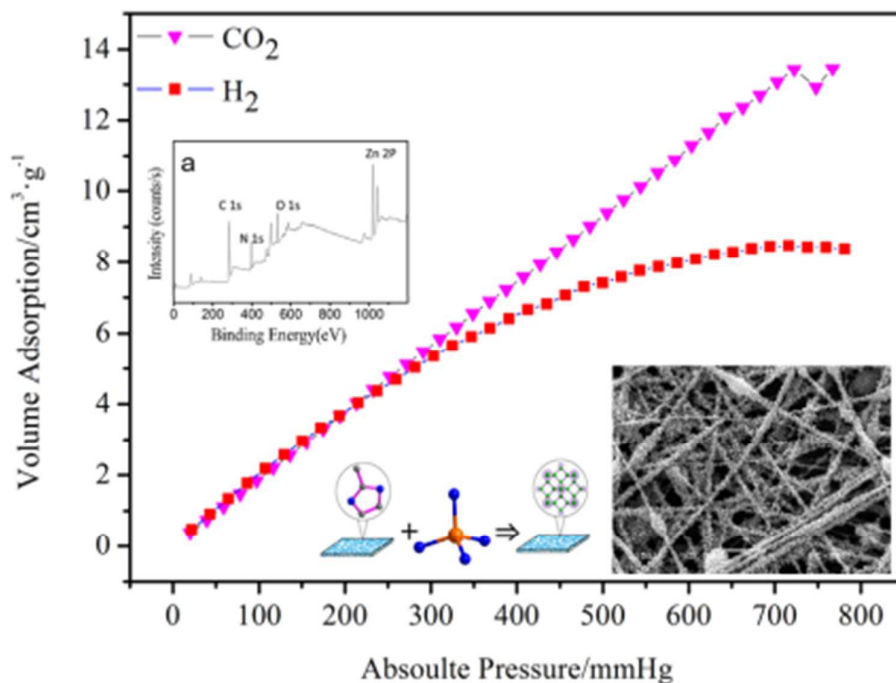
Polymer-Metal organic framework Core-Shell framework Nanofibers via electrospinning and Their gas adsorption Activity

Ming Gao^{1,2}, Lingwang Zeng¹, Jun Nie¹, Guiping Ma^{1*}

¹Key Laboratory of carbon fiber and functional polymers, Ministry of Education, Beijing University of Chemical Technology, Beijing, 100029, P. R. China

² School of Petrochemical Engineering, Changzhou University, Changzhou, Jiangsu 213164, PR China

ABSTRACT: In this study, we have fabricated of PAN@ZIF-8 core-shell nanofibers by combining electrospinning techniques and MOF synthesis method. In the first step, 2MI which acted as the ligand was dispersed on PAN by using electrospinning technique, then through mutual coordination in zinc acetate solution which provide Zn^{2+} ion. In the second step, the nanofibers mats were immersed in ZIF-8 seed solution, and the continuous and compact ZIF-8 was formed on PAN surface through the second growth crystal. The images investigated by XPS, SEM and TEM revealed the core-shell structure of PAN@ZIF-8 nanofibers which have uniform nanoshell while the diameter of crystal were different. In addition, the core-shell PAN@ZIF-8 nanofibers have shown unique properties such as stable structural flexibility and excellent gas adsorption capability. Our findings suggest that core-shell PAN@ZIF-8 nanofiber mats can be a good candidate as a filter material for gas absorption properties along with ZIF-8 structural flexibility and stability.



KEYWORDS: electrospinning, nanofibers, ZIF-8, core-shell, gas adsorption.

Introduction

Zeolitic imidazolate frameworks (ZIFs) are an emerging subclass of metal-organic framework (MOF) materials that could serve as an effective platform for gas adsorption^[1], carbon dioxide separation^[2], catalysis^[3] and hydrogen storage^[4] due to their ordered structures, large internal surface areas, thermal stabilities and adjustable chemical functionality^[5]. Especially, ZIF-8 ($\text{Zn}(\text{2MI})_2$, 2MI=2-methylimidazole) is one of the most studied ZIFs featuring a crystallization cubic lattice with sodalite (SOD) topology. It is prepared by in situ and possesses excellent chemical and thermal stabilities, which is advantageous for membrane applications. Therefore, various substrates and techniques have been applied to prepare ZIF-8 films/membranes, such as $\alpha\text{-Al}_2\text{O}_3$ ^[6], nanofiber^[7,8], etc. The electrospinning technique has become a versatile method for producing multifunctional nanofibers from various materials including

polymers, polymer blends, and composites, etc^[9-11]. More importantly, electrospun nanofibers have unique properties including a very high specific surface area, pore sizes within the nano range, high porosity and very lightweight since the fiber with diameters ranging from one micrometer down to a few tens of nanometers^[12]. The core-shell structure nanofibers as one of the most traditional and interesting nanostructures has attracted great attention due to it has been successfully applied in various fields, such as gas purification, catalysts support, pervaporation liquid chromatography, and information storage^[13-17].

In this work, we report a facile and scalable strategy to obtain integrated, binder-free, flexible PAN@ZIF-8 core-shell nanofibers mats, which shows remarkable gas absorption properties due to their unique morphological features including high surface area and nanoporosity. Firstly, electrospinning has gained growing interest in the past decade because this technique is quite versatile and cost-effective for producing multifunctional nanofibers with variety of materials including polymers, polymer blends, metal oxides, composite structures as well as nonpolymeric systems, etc^[18-25]. Four different types of inorganic materials with different functional MOF were employed for the formation of composites and applied as functional materials^[26-28]. Particularly, since 2011, Rainer Ostermann and his co-workers have published the synthesis and characterization of ZIF-8/organic polymer nanofibers for the first time^[29]. However, Few scientists has tried to generate hierarchical ZIF-8 nanostructures by electrospinning techniques^[30,31]. In this way, we have successfully achieved integrated nanofibers based on the ZIF-8 nanocrystal growth along the fibers formed the continuous and compact ZIF-8 sheath. Moreover, the control of the fiber surface morphology and ZIF-8 nanocrystal orientation growth along the nanofiber is quite feasible for obtaining multifunctional electrospun nanofibers.

Herein, by using ZIF-8 as an example, the 2MI/PAN nanofibers were obtained by electrospinning, and then mutual coordination chelate with Zn^{2+} ion which provide by zinc acetate. After that, through the second growth crystal, the continuous and compact ZIF-8 was formed on the surface of PAN. Starting from this strategy, a uniform distribution of the MOF seeds were achieved. Free-standing flexible HKUST-1 and ZIF-8 membranes were obtained by Wu et al^[32,33] after the secondary growth step.

The core-shell structure PAN@ZIF-8 has the obvious advantages. Firstly, Polymer-MOFs composite nanofiber structures have intriguing properties which combine the advantages of polymers and MOFs such as structural flexibility, light weight, high thermal stability, excellent adsorption, hydrogen storage, catalytically properties, etc. Secondly, the surface gathering of 2MI during electrospinning of 2MI/PAN blending nanofiber can replace traditional pretreatment the PAN nanofibers to grow ZIF-8 crystals. Thirdly, the ZIF-8 nanocrystals grown along the fibers formed the continuous and compact ZIF-8 shell. When it was applied as gas absorption material, the as-synthesized core-shell PAN@ZIF-8 has high gas adsorption capacity.

Figure 1 shows the fabrication process of the integrated core-shell PAN@ZIF-8 grown on PAN nanofiber. Initially, a spot of ZIF-8 were grown on the PAN substrate due to the Mutual coordination chelate of 2MI and zinc ions. After the second growth, the ZIF-8 crystals grown along the fibers formed the continuous and compact ZIF-8 sheath.

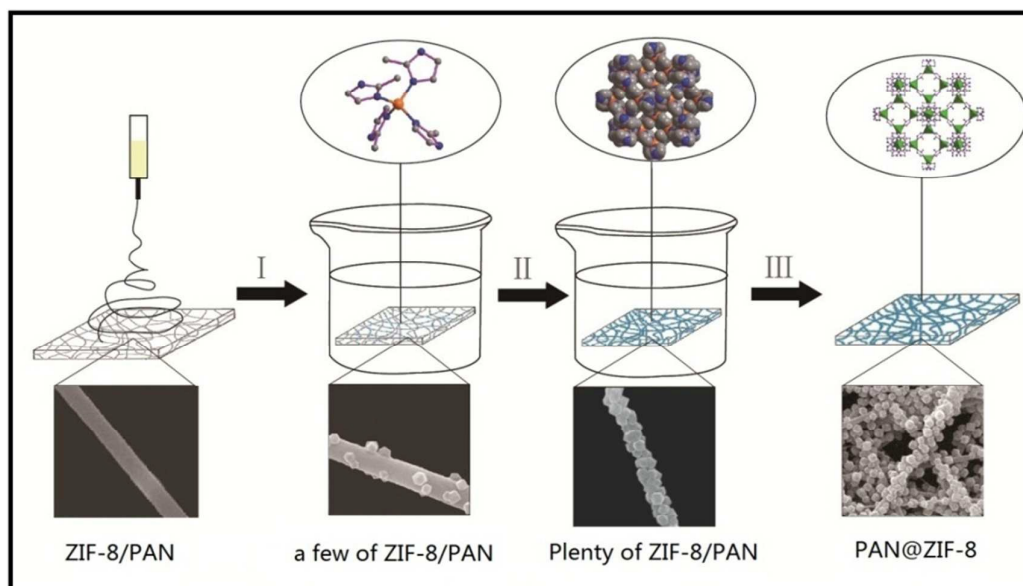


Figure 1. Schematic illustrating the synthesis procedures of PAN@ZIF-8 core-shell.

Experimental Section

Chemicals: All the chemicals were of analytical grade and used as received without further purification. Typically, Polyacrylonitrile (PAN, MW=9,000, Beijing Yili Fine Chemical), Zinc acetate dehydrate ($\text{Zn}(\text{OAc})_2 \cdot 2\text{H}_2\text{O}$, 99% purity, Sigma), 2-methylimidazole, N,N-dimethylformamide (DMF, 99.5%, Tianjin Chemicals), 2-methylimidazole (2MI, 99%, Aladdin).

Preparation of the 2MI/PAN flexible substrates: 2MI/PAN substrates were prepared via blending imidazolate into electrospinning solutions. A vertical-axis electrospinning installation was used to electrospin a mixed solution including PAN (1g), 2MI (1mmol) and N,N-dimethylformamide (11g). The electrospun fibers were collected on a grounded aluminum foil.

Synthesis of the Core-Shell PAN@ZIF-8: The nanocrystals on the PAN fiber surface were prepared by adding the 2MI/PAN substrates into the solution of

Zn(OAc)₂·2H₂O (0.5 mmol) dissolved in 40ml methanol at 60°C for 2h. Then the products were washed with methanol for several times. For the synthesis of the core-shell PAN@ZIF-8, the growth solution was prepared by adding MI, zinc acetate and methanol solution at 60°C. Especially, the mole ratio of 2MI, zinc acetate and methanol were 1:4:625 and 1:2:625, respectively. Finally, synthesis of the core-shell PAN@ZIF-8 was activated by removing the solvent under vacuum for 12h at room temperature.

Characterization

The samples were determined by X-ray diffraction (XRD; Rigaku D/MAX-YA) using Cu K α radiation, $\lambda = 0.154$ nm, scans were performed from (2 θ) 3-50° by rate 5/min. Scanning electron microscopy (SEM; JSM-6360LA, Japan) at an acceleration voltage of 15 kV. Transmission electron microscopy (TEM; JEM-2100, Japan) operated at 200 kV accelerating voltage. The electrospun fibers were dispersed in DMF and then dip-coated onto the copper grids. The specimens were conducted using an XPS system (XPS, Thermo Electron Corporation, Escalab 250, Germany). The photoelectron take-off angle is 45 with respect to the sample plane. Survey spectra were run in the binding energy range 0-1300eV and high-resolution spectra of Zn1s, O1s, and N1s were collected. The N₂ adsorption-desorption isotherm measurements were carried out on a Micromeritics ASAP2010 analyzer at 77 K. Prior to the measurement, the sample was degassed at 120°C for 6 h in the vacuum line. The gas adsorption was tested by the same device (ASAP2020) with the same pretreatment method but 20 °C.

Results and discussion

The XRD patterns of pristine ZIF-8 nanocrystal and core-shell PAN@ZIF-8

nanofibers are given in Figure 2. The presence of strong peaks implies a high crystallinity of the prepared ZIF-8 which are in good agreement with previous experimental works^[34]. Where the peaks at $2\theta = 7.30, 10.35, 12.70, 14.80, 16.40$ and 18.00 correspond to planes (110), (200), (211), (220), (310), and (222), respectively. In the figure 2a shows the X-ray diffraction (XRD) pattern of the as-synthesized product. The diffraction peaks matched well with the simulated XRD pattern of ZIF-8 according to the published crystal structure data^[35], indicating that the as-synthesized ZIF-8 was pure-phase. The considerably high patterns of PAN@ZIF-8 nanofiber mats Figure 2b with the simulated sample also shows that the ZIF-8 nanocrystals grown along the fibers formed the continuous and compact ZIF-8 sheath. Figure (2 right) represents the SEM image of the core-shell PAN@ZIF-8 nanofiber. The prepared ZIF-8 nanocrystal on the surface of PAN nanofiber possesses rhombic dodecahedron morphology which show good agreement with the literature^[34]. The different particle size of the prepared samples was measured by nanomeasurer 1.2 shows in (Figure S2). Besides, The FTIR analysis (see Figure S1) reveals that ZIF-8 nanocrystal successful fabricated on the PAN fiber.

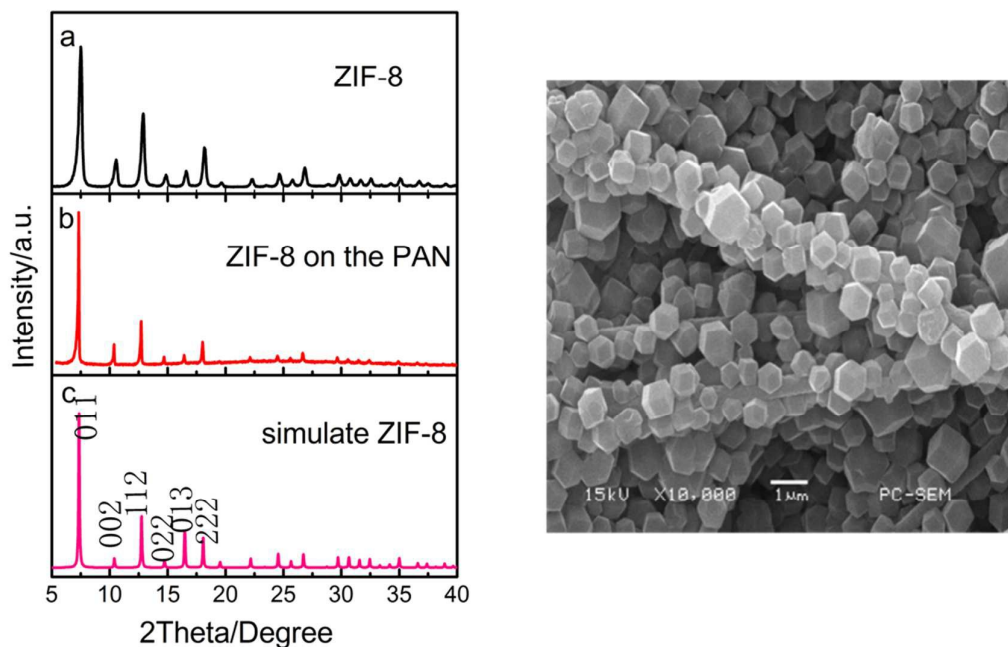


Figure 2.left: XRD patterns of the ZIF-8(a), PAN@ZIF-8 (b), and a simulated ZIF-8 (c).Right: morphology of the prepared PAN@ZIF-8.

Morphology of the core-shell PAN@ZIF-8 nanofibers. SEM images reveal the ZIF-8 nanocrystals grown along the fibers, which was formed the continuous and compact ZIF-8 shell. The 2MI/PAN were fabricated via blending spinning 2MI and PAN with N,N-dimethylformamide. In this strategy, the 2MI/PAN surface served as the ZIF-8 nanocrystals growth template provided the ligand and the Zn^{2+} ions provided by dissolving zinc acetate with methanol. As obviously seen from the scanning electron microscopy (SEM) images (Figure 3a), uniform ZIF-8 adhering on the PAN substrate, resulting in a stronger adhesive force which was well solved the problem of fiber surface pretreatment^[36]. Figure 3(b and c) shows the SEM images of core-shell PAN@ZIF-8 nanofibers obtained at 1:4:625 and 1:2:625(in mole ratio) of MI, zinc acetate and methanol, respectively. From figure 3c, we can see that the grain diameter of ZIF-8 nanocrystals was about 614 nm which was larger than that of in

figure 3b (206 nm). The increasing size was resulted from the different concentration of MI, zinc acetate. As shown in (Figure 3b,c), the PAN surface was still completely covered by the ZIF-8 nanocrystals which grow along the fibers and well-aligned formed the continuous and compact ZIF-8 sheath after two-step reaction^[32].

It is worth mentioning that the PAN@ZIF-8 synthesized remained intact after twenty minutes of ultrasonic vibration, indicating good bonding strength between the crystal layer and substrate^[37]. More important, the morphologies of the core-shell PAN@ZIF-8 nanofibers were further investigated by TEM (see Figure S3). This results show that the ZIF-8 shell layer possess of uniform thickness on the PAN fiber surface.

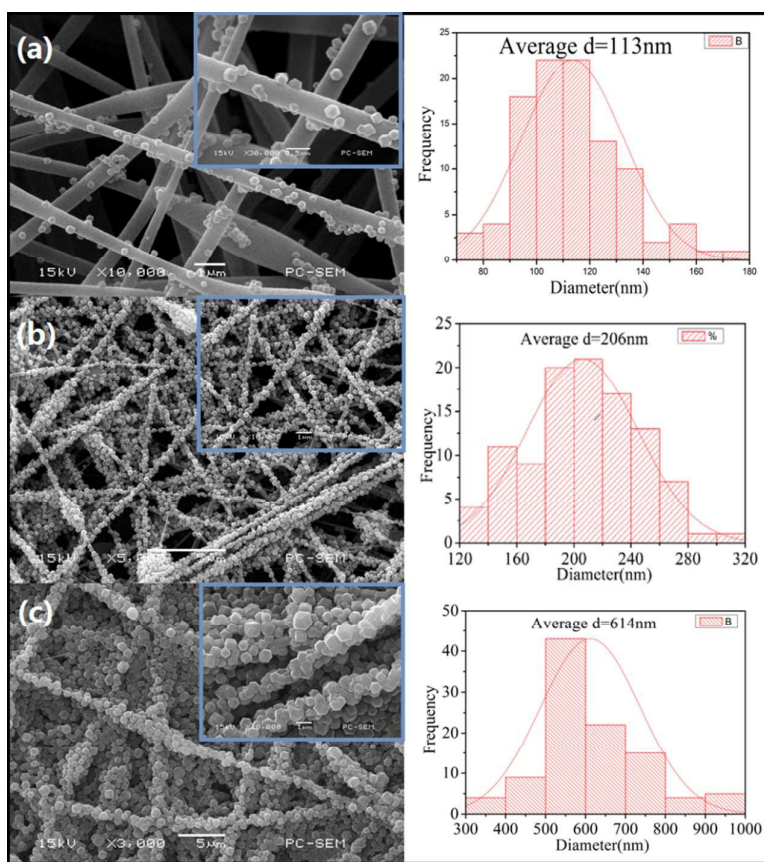


Figure 3. SEM images for synthesis of ZIF-8 on PAN; (a) ZIF-8 on the PAN, (b, c) the core-shell PAN@ZIF-8 nanofibers at 1:4:625 and 1:2:625(in mole ratio) of MI, zinc acetate and methanol

Surface analysis of the core-shell PAN@ZIF-8 nanofibers. Surface chemical composition and bonding states of the pristine ZIF-8 nanofibers and core-shell PAN@ZIF-8 nanofibers were investigated by using XPS.

Table 1. Atomic Concentrations Generated from XPS Wide Energy Survey Scans

Samples	C(%)	O(%)	Zn(%)	N(%)	
ZIF-8		62.5	11.89	7.84	17.77
PAN@ZIF-8		69.26	8.55	5.73	16.46

Table 1 summarizes the compositional data of pristine ZIF-8nanocrystal and core-shell PAN@ZIF-8 nanofibers in atomic concentrations. As anticipated, all expected ZIF-8 features were observed, including zinc(coordinating metal), nitrogen, and carbon (imidazole linker)^[38] (See Figure S4).Usually, the probe depth for XPS is approximately the top atomic layers (~ 10 nm)^[39] depending on the take off angle between the photoelectrons and the sample surface. Due to the average diameter of the ZIF-8 nanoparticles is 34.0 ± 2.9 nm so that the core of PAN was not observed in Figure 4.From the Figure 4a an oxygen signal was observed due to ambient exposure during sample preparation as reactions are possible between undecoordinated Zn sites, CO₂, and water in air^[40].

To obtain quantitative chemical information on the PAN@ZIF-8 nanofiber, multiple regions were scanned with higher resolution, including Zn 2p, O 1s, N 1s,

and C 1s, as shown in Figure 4 (bottom). To determine the nature of the surface terminations, we began by fitting the N 1s region, obtaining a good fit using two peaks: a main peak at 400.5eV was shown in Figure 3(a), which we assigned to the imidazole groups based on comparison to analogous species^[41,42], which were found to be almost stoichiometric as expected. On the other hand, the absence of nitrogen peak in the XPS survey scans for core-shell PAN@ZIF-8 nanofibers indicated that the surface of the PAN nanofibers were successfully coated by ZIF-8 layer. Formation of zif-8 nanocrystal on the surface of PAN nanofibers was also confirmed by Zn 2p high resolution XPS scan (Figure 4d). Zn 2p_{3/2} and Zn 2p_{1/2} subpeaks of the Zn 2p doublet located at 1021.73 and 1044.76eV, which is compatible with Zn2p of the ZIF-8 structure seen in crystals of this MOFs^[43].

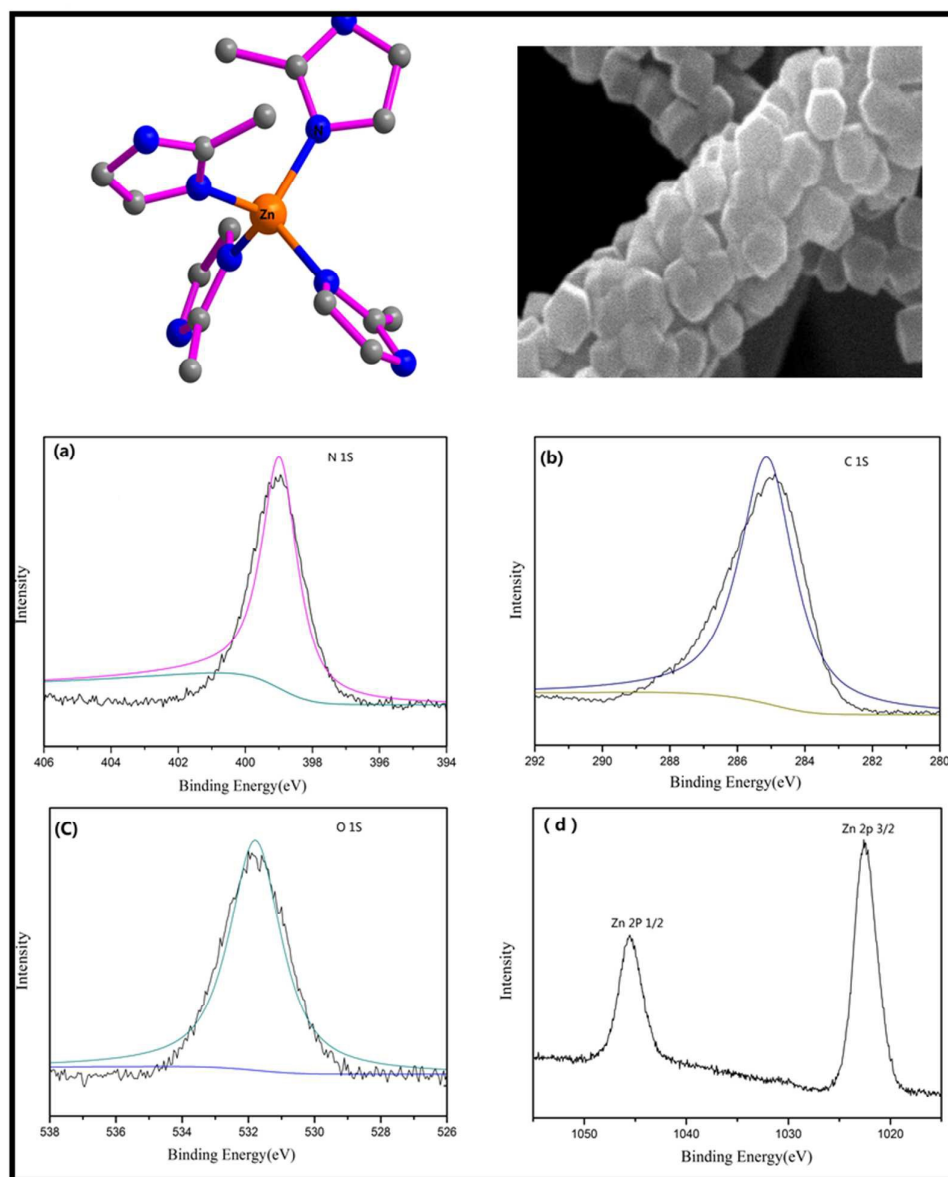


Figure 4. Top: ZIF-8 structures and core-shell PAN@ZIF-8 nanofiber. Bottom: High-resolution XPS spectra of core-shell PAN@ZIF-8 nanofiber mats: (a) N 1s, (b) C 1s, (c) O 1s, and (d) Zn 2p regions.

Specific surface area analysis of the core-shell PAN@ZIF-8 nanofibers. The adsorption properties of PAN@ZIF-8 nanofibers were measured by the N₂ adsorption curves and micropore analysis. The results of pure ZIF-8 nanocrystalline, 2MI/PAN nanofiber and core-shell ZIF-8@PAN are compared in Figure 5 and Table 2, which

indicated a type I isotherm. The high nitrogen adsorption at very relative low pressures is due to the presence of micropores^[44]. Micropore volume of the resulting 2MI/PAN, ZIF-8 nanocrystal and core-shell PAN@ZIF-8 nanofiber are about 0.0005, 0.62 and 0.51 cm³g⁻¹/g, respectively. The specific surface area of 2MI/PAN, pure ZIF-8 nanocrystal and the core-shell PAN@ZIF-8 nanofiber are 5, 1219 and 983 m²g⁻¹. The specific surface area of pure ZIF-8 nanocrystal is higher than the core-shell PAN@ZIF-8 nanofiber, which is due to the PAN have low specific surface area existence in ZIF-8 nanocrystal layers. Compared with previous the result of Zhou lian^[36]. In our strategy, which based on 2MI/PAN substrate exhibited a much higher gas adsorption capacity. In a word, the 1D electrospun PAN nanofibers is contributed to the orderly growth of ZIF-8 nanocrystal along the nanofibers orientation formed the core-shell PAN@ZIF-8 nanofiber and avoided the large area aggregation of nanocrystals.

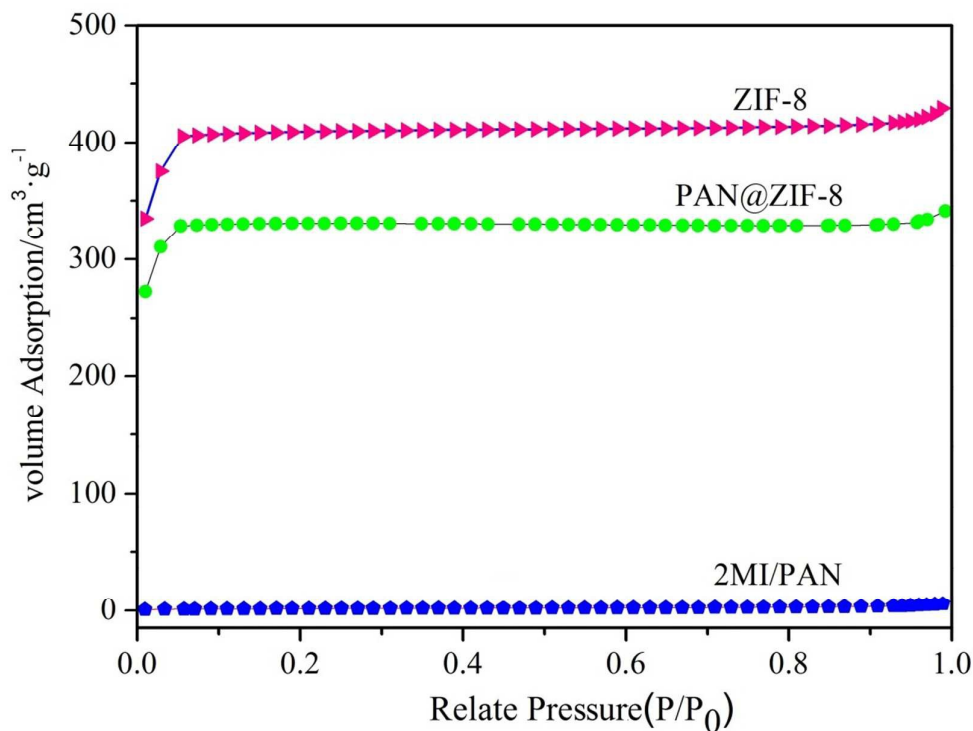


Figure 5. N_2 adsorption-desorption analysis of ZIF-8, PAN@ZIF-8 and 2MI/PAN.

Table 2 N_2 adsorption-desorption data

Sample	Surface area ($m^2 g^{-1}$) ^a	Micropore volume ($cm^3 g^{-1}$) ^b
ZIF-8	1219	0.62
PAN@ZIF-8	983	0.51
2MI/PAN	5	0.0005

^aAccording to the BET model. ^b According to the t-plot model.

Gas adsorption of the core-shell PAN@ZIF-8 nanofibers. Here, we demonstrate that the core-shell PAN@ZIF-8 nanofiber mat can be a very good candidate as filtering material because of the flexible polymeric core and the gas adsorption of the ZIF-8 shell layer. These nanofiber mats can be easily handled and folded as a

free-standing material. We have tested the gas adsorption of the core-shell PAN@ZIF-8 nanofiber mats by following the gas adsorption which was used the ASAP2020 at 20 °C which possess good CO₂ and H₂ adsorption performance. From the Figure 6, at 800 mmHg, the volume of adsorption for H₂ and CO₂ is 8.1 and 13.3 cm³g⁻¹, respectively. It is clear that the adsorption capacity of PAN@ZIF-8 for CO₂ is much higher than that of H₂. It probably has potential application in preferential CO₂ adsorption membranes. These materials combining the excellent toughness of PAN nanofibers with the outstanding adsorption ability of ZIF-8 have prospective applications in air-purifying clothes.

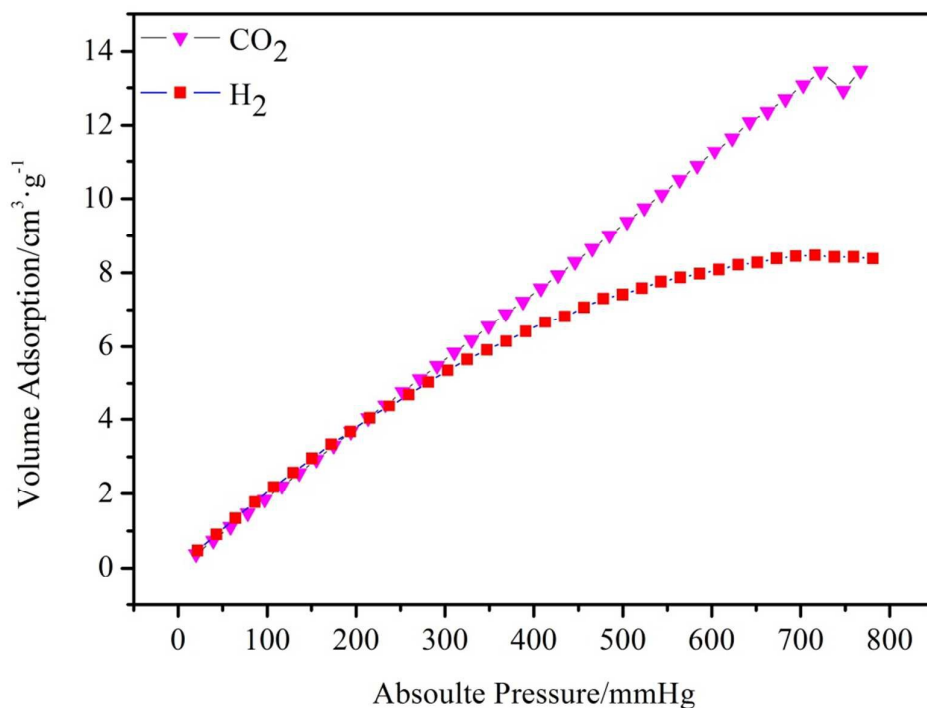


Figure 6. Gas adsorption isotherms of PAN@ZIF-8 at room temperature (20 °C)

CONCLUSIONS

In conclusion, we have successfully fabricated core-shell PAN@ZIF-8 nanofibers

based on 2MI/PAN for the first time. In our strategy, the imaging analyses by SEM, TEM and XPS revealed the continuous and compact core-shell structure of PAN@ZIF-8 nanofibers. By N₂ adsorption-desorption, core-shell PAN@ZIF-8 shows a high surface area of 983 cm²g⁻¹. In addition, the core-shell PAN@ZIF-8 volume of adsorption capacity for CO₂ and H₂ are 13.3 and 8.1 cm³g⁻¹, respectively. Our results indicate that core-shell PAN@ZIF-8 nanofiber mats can be quite applicable as a filtering/membrane material for treatment of gas adsorption. Consequently, based on the 2MI/PAN flexible substrates, the core-shell PAN@ZIF-8 nanofibers can be fabricated for many applications including filters/membranes, catalyst supports, air purification, gas sensors and special gas adsorption.

Reference:

- [1] D. D. Ge and H. K. Lee, Sonication-assisted emulsification microextraction combined with vortex-assisted porous membrane-protected micro-solid-phase extraction using mixed zeoliticimidazolate frameworks-8 as sorbent, *J. Chromatogr. A*. 2012,1263:1-6.
- [2] R. Li, X. Q. Ren, X. Feng, X. G. Li, C. W. Hu and B. Wang, A highly stable metal-and nitrogen-doped nanocomposite derived from Zn/Ni-ZIF-8 capable of CO₂ capture and separation, *Chem. Commun.* 2014, 50: 6894-6897.
- [3] M. Zhu, M. A. Carreon, D. Srinivas, S. Bhogeswararao, P. Ratnasamy, Catalytic activity of ZIF-8 in the synthesis of styrene carbonate from CO₂ and styrene oxide, *Catal. Commun.* 2013, 32: 36-40.
- [4] W. Hui, Z. Wei and Y. Taner, Hydrogen Storage in a Prototypical Zeolitic Imidazolate Framework-8, *J. Am. Chem. Soc.* 2007, 129: 5314-5315.
- [5] Y. Hu, Z. X. Liu, J. Xu, Y. Huang, Y. Song, Evidence of Pressure Enhanced CO₂

- Storage in ZIF-8 Probed by FTIR Spectroscopy, *J. Am. Chem. Soc.* 2013, 135: 9287–9290.
- [6] M. C. McCarthy, V. Varela-Guerrero, G. V. Barnett and H.-K. Jeong, Synthesis of Zeolitic Imidazolate Framework Films and Membranes with Controlled Microstructures. *Langmuir*, 2010, 26: 14636–14641.
- [7] V. I. Isaeva, M. I. Barkova, L. M. Kustov, D. A. Yrtsova, E. A. Efimov and V. V. Teplyakov, In situ synthesis of novel ZIF-8 membranes on polymeric and inorganic supports, *J. Mater. Chem. A*. 2015, 3, 7469–7476.
- [8] Hyuk Taek Kwona and Hae-Kwon Jeong, Highly propylene-selective supported zeolite-imidazolate framework (ZIF-8) membranes synthesized by rapid microwave-assisted seeding and secondary growth, *Chem. Commun.*, 2013, 49: 3854–3856.
- [9] Z. H. Guo, S. Y. Wei, H. L. Qu, Coaxial Electrospun Nanostructures and Their Applications, *J. Mater. Chem. A*. 2013, 1: 11513–11528.
- [10] J. H. Zhu, S. Y. Wei, R. Patil, Rutman, D.; Kucknoor, A. S.; Wang, A.; Guo, Z. H. Ionic Liquid Assisted Electrospinning of Quantum Dots/Elastomer Composite Nanofibers, *Polymer* 2011, 52: 1954–1962.
- [11] M. J. Chen, H. L. Qu, J. H. Zhu, Z. P. Luo, A. Khasanov, A. S. Kucknoor, N. Haldolaarachchige, D. P. Young, S. Y. Wei, Z. H. Guo, Magnetic Electrospun Fluorescent Polyvinylpyrrolidone Nanocomposite Fibers, *Polymer* 2012, 53: 4501–4511.
- [12] S. Ramakrishna, K. Fujihara, W. E. Teo, T. Yong, Z. W. Ma and R. Ramaseshan, electrospun nanofibers: solving global issues, *Mater. Today*, 2006, 9: 40–50.
- [13] M. Rose, B. Böhringer, M. Jolly, R. Fischer and S. Kaskel, MOF Processing by Electrospinning for Functional Textiles, *Adv. Eng. Mater.* 2011, 13: 356–360.

- [14] M. M. Zhang, Y. B. Yang, C. Li, Q. Liu, C. T. Williams and C. H. Liang, PVP-Pd@ZIF-8 as highly efficient and stable catalysts for selective hydrogenation of 1,4-butanediol, *Catal. Sci. Technol.* 2014, 4: 329-332.
- [15] Alina Kudasheva, Sara Sorribas, Beatriz Zornoza, Carlos Téllez and Joaquín Coronas, Pervaporation of water/ethanol mixtures through polyimide based mixed matrix membranes containing ZIF-8, ordered mesoporous silica and ZIF-8-silica core-shell spheres, *J. chem. technol. biot.* 2015, 90: 669-677.
- [16] Dr. Yan-Yan Fu, Dr. Cheng-Xiong Yang and Prof. Dr. Xiu-Ping Yan. Fabrication of ZIF-8@SiO₂ Core-Shell Microspheres as the Stationary Phase for High-Performance Liquid Chromatography, *Chem-Eur. J.* 2013, 19: 13484-13491.
- [17] L. Pan, Z. H. Ji, X. H. Yi, X. J. Zhu, X. X. Chen, J. Shang, G. Liu, and R. W. Li, Metal-Organic Framework Nano film for Mechanically Flexible Information Storage Applications, *Adv. Funct. Mater.* 2015, 25: 2677-2685
- [18] X. Lu, C. Wang, Y. Wei, One-Dimensional Composite Nanomaterials: Synthesis by Electrospinning and Their Applications, *Small.* 2009, 5: 2349-2370.
- [19] S. Ramakrishna, R. Jose, P. S. Archana, A. S. Nair, R. Balamurugan, J. Venugopal, W. E. Teo. Science and engineering of electrospun nanofibers for advances in clean energy, water filtration, and regenerative medicine. *J. Mater. Sci.* 2010, 45: 6283-6312.
- [20] R. J. Wade, E. J. Bassin, W. M. Gramlich, and J. A. Burdick, Nanofibrous Hydrogels with Spatially Patterned Biochemical Signals to Control Cell Behavior, *Adv. Mater.* 2015, 27: 1356-1362.
- [21] Andreas, Greiner, and H. Joachim, Wendorff, Electrospinning: A Fascinating

- Method for the Preparation of Ultrathin Fibers, *Angew. Chem.* 2007, 46: 5670-5703.
- [22] W. E. Teo, S. Ramakrishna, Electrospun nanofibers as a platform for multifunctional, hierarchically organized nanocomposite, *Compos. Sci. Technol.* 2009, 69: 1804-1817.
- [23] S. Agarwal, A. Greiner, On the way to clean and safe electrospinning—green electrospinning: emulsion and suspension electrospinning, *Polym. Adv. Technol.* 2011, 22: 372-378.
- [24] A. Celebioglu, T. Uyar, Electrospinning of nanofibers from non-polymeric systems: polymer-free nanofibers from cyclodextrin derivatives, *Nanoscale* 2012, 4: 621-631.
- [25] F. Kayaci, C. Ozgit-Akgun, I. Donmez, N. Biyikli, T. Uyar, Polymer–Inorganic Core–Shell Nanofibers by Electrospinning and Atomic Layer Deposition: Flexible Nylon–ZnO Core–Shell Nanofiber Mats and Their Photocatalytic Activity, *ACS Appl. Mater. Interfaces* 2012, 4: 6185–6194.
- [26] Z. C. Zhang, Y. F. Chen, S. He, J. C. Zhang, X. B. Xu, Y. Yang, F. Nosheen, F. Saleem, W. He and X. Wang. Hierarchical Zn/Ni-MOF-2 Nanosheet-Assembled Hollow Nanocubes for Multicomponent Catalytic Reactions, *Angew. Chem. Int. Ed.* 2014, 53: 12517–12521,
- [27] M. Pang, A. J. Cairns, Y. Liu, Y. Belmabkhout, H. C. Zeng, M. Eddaoudi, Synthesis and Integration of Fe-soc-MOF Cubes into Colloidosomes via a Single-Step Emulsion-Based Approach, *J. Am. Chem. Soc.* 2013, 135: 10234–10237.
- [28] K. Okada, R. Ricco, Y. Tokudome, M. J. Styles, A. J. Hill, M. Takahashi and P. Falcaro, Copper Conversion into Cu(OH)₂ Nanotubes for Positioning Cu₃(BTC)₂ MOF Crystals: Controlling the Growth on Flat Plates, *3D*

- Architectures, and as Patterns, *Adv.Funct.Mater.*2014, 24: 1969–1977.
- [29] R. Ostermann, J. Cravillon, C. Weidmann, M. Wiebcke and B. M Smarsly, Metal–organic framework nanofibers via electrospinning, *Chem. Commun.*2011, 1: 442–444.
- [30]M. Rose, B.Böhringer, M. Jolly, R. Fischer and S. Kaskel, MOF Processing by Electrospinning for Functional Textiles,*Adv. Eng. Mater.*, 2011,13:356–360.
- [31]Y. X. Xu, Y. Q. Wen, W. Zhu, Y. N. Wu, C.X. Lin, G. T.Li, Electrospun nanofibrous mats as skeletons to produce MOF membranes for the detection of explosives, *Mater. Lett.*, 2012,87: 20-23.
- [32] Y. N. Wu, F. T. Li, H. M. Liu, W. Zhu, M.M.Teng, Y. Jiang, W. N.Li,D. Xu, D. H.He, P. Hannam and G. T. Li, Electrospun fibrous mats as skeletons to produce free-standing MOF membranes, *J. Mater. Chem.* 2012,22: 16971–16978.
- [33] M. Bechelany, M. Drobek, C. Vallicari, A. AbouChaaya, A. Julbe, P. Miele, Highly crystalline MOF-based materials grown on electrospun nanofibers, *Nanoscale*,2015, 7: 5794–5802.
- [34]A. F. Gross, E. Sherman and J. J. Vajo, Aqueous room temperature synthesis of cobalt and zinc sodalite zeoliticimidizolate frameworks, *Dalton Trans*, 2012, 41: 5458-5460.
- [35] J. A.Gee, J. Chung, S. Nair and D. S. Sholl, Adsorption and Diffusion of Small Alcohols in Zeolitic Imidazolate Frameworks ZIF-8 and ZIF-90, *J. Phys. Chem. C.* 2013, 117: 3169–3176.
- [36] L. Zhou Lu M. Hui andY.Ou, F. Zhao, In situ crystal growth of zeoliteic imidazolate frameworks (ZIF) on electrospun polyurethane nanofibers. *Dalton Trans*, 2014, 43: 6684–6688.
- [37] Li. L. Fan, M.Xue, Z. X. Kang, H. Li and S. L. Qiu, Electrospinning technology

- applied in zeoliticimidazolate framework membrane synthesis, *J. Mater. Chem.* 2012, 22: 25272–25276.
- [38] F. Y. Tian, A. Cerro, A. M. Mosier, H. Wayment-Steele, R.S. Shine, A. Park, E. R. Webster, L. E. Johnson, M. S. Johal, L. Benz, Surface and Stability Characterization of a Nanoporous ZIF-8 Thin Film, *J. Phys. Chem. C.* 2014, 118: 14449–14456.
- [39] M. P Seah, W. A. Dench, Quantitative Electron Spectroscopy of Surfaces: A Standard Data Base for Electron Inelastic Mean Free Paths in Solids, *Surf. Interface Anal.* 1979, 1:2–11.
- [40] C. Woll, The Chemistry and Physics of Zinc Oxide Surfaces, *Prog. Surf. Sci.* 2007, 82:55–120.
- [41] N. Liedana, A. Galve, C. Rubio, C. Tellez, J. Coronas, CAF@ZIF-8: One-Step Encapsulation of Caffeine in MOF, *ACS Appl. Mater. interfaces.* 2012, 4: 5016–5021.
- [42] G. Xue, Q. Dai, S. Jiang, Chemical Reactions of Imidazole with Metallic Silver Studied by the Use of SERS and XPS Techniques, *J. Am. Chem. Soc.* 1988, 110: 2393–2395.
- [43] R. L. Papparello, E. E. Miro, J. M. Zamaro, Secondary growth of ZIF-8 films onto copper-based foils. Insight into surface interactions, *Microporous. Mesoporous. Mater.* 2015, 211: 64-72.
- [44] M. He, J. F. Yao, Q. Liu, K. Wang, F. Y. Chen, H. T. Wang, Facile synthesis of zeolitic imidazolate framework-8 from a concentrated aqueous solution, *Microporous. Mesoporous. Mater.* 2014, 184: 55–60.